IEEE Access
Multidisciplinary | Rapid Review | Open Access Journal

Received June 4, 2019, accepted July 2, 2019, date of publication July 11, 2019, date of current version August 2, 2019.

Digital Object Identifier 10.1109/ACCESS.2019.2928321

Phase Modulation of Retro-Reflected Radar Echo Signal Using a Microstrip Van-Atta Array

KUNPENG SONG[1], DEJUN FENG[1], JUNJIE WANG[1], QIANPENG XIE[2], AND LEI LIU[2]

[1]State Key Laboratory of Complex Electromagnetic Environmental Effects on Electronics and Information System, National University of Defense Technology, Changsha 410073, China

[2]College of Electrical Science, National University of Defense Technology, Changsha 410073, China

Corresponding author: Dejun Feng (fdj117@sina.com)

This work was supported in part by the National Natural Science Foundation of China under Grant 61701507 and Grant 61571451.

ABSTRACT Van-atta array is able to retro-reflect the incident signal back to the income direction and, thus, it can maintain a relatively larger radar cross-section (RCS) in a large range of incidence angles. The previous researches about van-atta array focus mainly on satellite communication and radio frequency identification (RFID). In this paper, this retro-reflective characteristic of the van-atta array is further extended to radar signal processing in a large angle range. To accomplish this, a microstrip van-atta array with adjustable transmission line is designed to add phase modulation to the retro-reflected signal. The phase modulation is achieved through the incorporation of the microwave single-pole double-throw (SPDT) switches into the array structure, which provides the retro-reflected signal ability to switch between two transmission lines separating half a wavelength. As a result, the phase modulation of retro-reflected signal can be precisely realized in a large range angle. The advantage of the designed van-atta array is that it can realize phase modulation in a large range angle of the incident signal. The simulations and experimental results are utilized to verify the effectiveness of phase modulation produced by designed van-atta array.

INDEX TERMS Van-atta retro-reflective array, phase modulation, microstrip patch array, single-pole double-throw (SPDT) switch.

I. INTRODUCTION

Phase modulation of radar echo signal is an efficient radar jamming strategy and has attracted great attention. The traditional phase modulation strategy is mainly performed by active radar jamming system in which the jammer intercepts victim radar pulse, modulates this pulse, and retransmits this altered pulse (modulated signal) back to the victim radar [1]–[3]. However, to achieve high coherence of repetitive signals, it needs to sample the signal accurately and storage the digital signal using digital radio frequency memory (DRFM) and other complex system. This is difficult in implementation and can not be processed timely [4].

On the contrary, passive strong scatterer with the incorporation of dynamic elements can also realize phase modulation without complex memory system, which is flexible, diversity and easily accomplished. Recently, the phase switched screens (PSS) have been explored for the possibility of phase modulation of radar echo signal [5]–[8]. By applying a PIN diode and excitation current to the active screen, PSS can apply phase intermittent modulation to the reflected signal. PSS-based phase modulation can achieve good performance when the signal is incident vertically. However, in the case of oblique incidence of the signal, the phase modulation accuracy suffers severe attenuation. Besides, while signal obliquely incident on PSS plane, the phase modulated signal will be reflected to the symmetrical direction due to specular reflection so that the modulated signal can not be received by radar receiver and form effective jamming to victim radar.

The van-atta array, first introduced by L. C. Van Atta, can maintain a relatively larger radar cross-section (RCS) in a large range of incidence angles [9]–[11] and is widely used in satellite communication and radio frequency identification (RFID). Since van-atta array retro-reflector is able to return the incident signal back to the income direction automatically, it can act as an ideal radar jammer in radar echo signal modulation. Moreover, the van-atta array can also achieve the energy amplification of the incident signal by embedding an amplifier in the interconnected transmission line [12]. To achieve dynamic adjustment and echo signal modulation,

The associate editor coordinating the review of this manuscript and approving it for publication was Chengpeng Hao.

the PIN diode is always embedded in the interconnection transmission line of van-atta array [13]. Therefore, the scattering characteristics of van-atta retro-reflector can be controlled through changing the on and off state of the PIN diode. Besides, the microwave SPDT switch [14]–[16] can be attached to the interconnection transmission line of van-atta array to switch the retro-reflected signal going through two different transmission lines. Since the phase delay of retro-reflected signal is determined by the length of transmission line, phase modulation can be accomplished by switching the length of transmission line using SPDT switch.

In this paper, planar antennas and printed transmission lines with SPDT switch accomplished by microstrip are used to implement a phase adjustable van atta retro-reflectors. To accomplish this, a unique series-fed microstrip patch arrays antenna [17], [18] is designed and implemented with minimal cross coupling among elements. The symmetrical antennas are connected with equal electrical length microstrip ground coplanar waveguide (GCPW) [19], [20] lines, thus making up the van-atta array. This compact array has a relatively large radar cross section (RCS) while maintaining the desired retro-reflectivity in the wide-angle range. Besides, the incorporation of the microwave single-pole double-throw (SPDT) switches into the array structure provide the retro-reflected signal ability of switching between two transmission lines separating half a wavelength. As a result, the phase of retro-reflected signal can be precisely switched from 0 to π by applying bias voltage to the SPDT switch. Using a square wave as the bias voltage can realize phase modulation of retro-reflected signal and after modulated, the retro-reflected signal can generate a series of symmetrical false targets in radar high-resolution range profile (HRRP). The rest of this article is organized as follows. In Section II, the Van-atta array and the method of phase reverse with microstrip SPDT switches and transmission lines are described in detail. In Section III, the microstrip van-atta array is designed in detail and the RCS characteristics of it is analyzed. In Section IV, the SPDT switch is designed and embedded in the van-atta array, and phase of retro-reflected signal in on and off bias voltage is displayed. In Section V, the measurement of designed van-atta array is conducted and discussed. Finally, the Section VI draws conclusions.

II. PRINCIPLE OF PHASE MODULATION BY VAN-ATTA RETRO-REFLECTIVE ARRAY

Van-atta array can automatically retro-reflect the signal to the incoming wave direction without any digital signal processing. The array consists of even symmetrical antennas. The two antennas symmetrical with each other are connected by an equal electrical length transmission line. The antenna is distributed symmetrically with equal interval aside the center of the array. As shown in Fig. 1, each antenna element both receives and emits signals and the received signal is emitted to symmetrical antenna elements after going through the transmission line. The lengths of the transmission lines connecting the antennas are equal or integer multiples of the wavelength

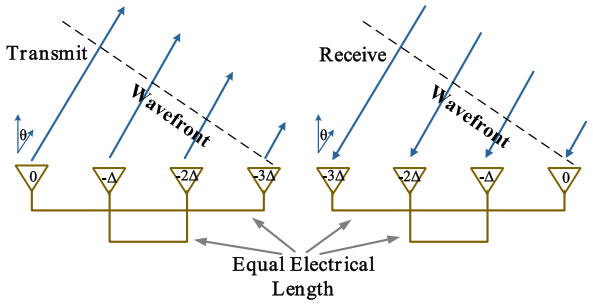

FIGURE 1. Schematic diagram of van-atta retro-reflective array.

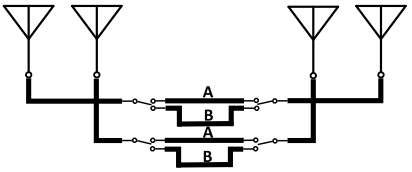

FIGURE 2. Van-atta array with microwave SPDT switch and two different transmission line.

difference, so that the incident wave and the retro-reflected wave have the same wavefront, and the retro-reflected signal can be returned to the same direction of incident signal.

The phase modulation is realized by changing the length of the transmission line. The microwave single-pole double-throw (SPDT) switch is turned to A or B route to realize the signal passing through two different transmission lines. The electrical length disparity between transmission line A and B is a half wavelength, so that the phase delay disparity of the signal passing through the two transmission lines is π.

When the A channel is turned on, the pulse signal retro-reflected through the Van-atta array can be described as:

$$s_A(t) = \text{rect}\left(\frac{t}{T_p}\right) s(t) \cos(2\pi f_c t) \tag{1}$$

where T_p is the pulse width, $s(t)$ is baseband radar signal and f_c is the carrier frequency. When the switch is turned to B channel, the signal retro-reflected through the Van-atta array is delayed half a wavelength relative to that of the A channel, and the retro-reflected signal is delayed $\Delta t = T_c/2$ more than that of A channel. Where T_c is the carrier signal period. Since the delay is only a half-period at high frequency, its effect on the low frequency baseband signal $s(t)$ and rect$(\cdot)$ envelope is negligible. The retro-reflected signal through B channel can be described as:

$$\begin{aligned} s_B(t) &= s_A(t + \Delta t) \\ &= \text{rect}\left(\frac{t + \Delta t}{T_p}\right) s(t + \Delta t) \cos(2\pi f_c (t + \Delta t)) \\ &\approx \text{rect}\left(\frac{t}{T_p}\right) s(t) \cos(2\pi f_c t + \pi) \\ &= -s_A(t) \end{aligned} \tag{2}$$

It can be obtained that by controlling the switch to A or B channel, we can realized the phase delay from 0 to π, thus

realizing the phase reversion and reflection coefficient of the retro-reflected signal 1 and −1. Switching the SPDT between A and B channel periodically can realize periodic phase modulation of the retro-reflected signal.

III. PASSIVE PLANAR VAN-ATTA ARRAY DESIGN

In this section, a passive planar microstrip van-atta array is designed. The 8 resonant series-fed microstrip patch array antennas connected with equal electrical length microstrip ground coplanar waveguide (GCPW) lines makes up the van-atta array. The designed van-atta array has a relatively large radar cross section (RCS) while maintaining the desired retro-reflectivity in the wide-angle range. Compared to flat metallic plate with equal size, the van-atta array can maintain a relatively larger RCS in the range of −40° to −40°. And the main RCS disparity between the van-atta array and the flat metallic plate is under the condition of oblique incidence. This difference is due to the retro-reflective characteristic of the van-atta array.

A. RESONANT SERIES-FED RECTANGULAR MICROSTRIP PATCH ARRAY

To maximize the total array efficiency and get high gain of antenna, resonant series-fed rectangular microstrip patch array is applied as the signal antenna of van-atta array. As shown in Fig. 3, the 9 × 1 half-wavelength patches connected with series narrow microstrip lines make up the antenna. The interval of adjacent feds is λ_g, and this arrangement reduces radiation into the substrate and cross coupling among array-elements.

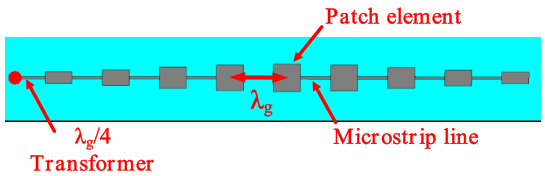

FIGURE 3. Resonant series-fed rectangular microstrip patch array.

The resonant series-fed patch array is terminated with an open circuit, which causes a standing wave across the array. The series array, from an equivalent circuit perspective, is the combination of parallel resonant circuits, each of which represents a single patch element. Each patch element act as series-fed radiators. For these patches to produce a single main lobe their standing wave currents should add in phase. To achieve this, the length of connecting microstrip lines are all $\lambda_g/2$. Since the elements are spaced a wavelength apart at resonance, their reactances theoretically cancel, leaving the parallel combination of input resistances. In order to achieve $Z = 50 + j0\ \Omega$ input impedance at 10GHz, the microstrip feed line connected to the edge of the first radiating patch incorporates a $\lambda_g/4$ transformer for impedance matching. The antenna is simluted using CST microwave studio and the characteristics of designed antenna are shown in Fig. 4.

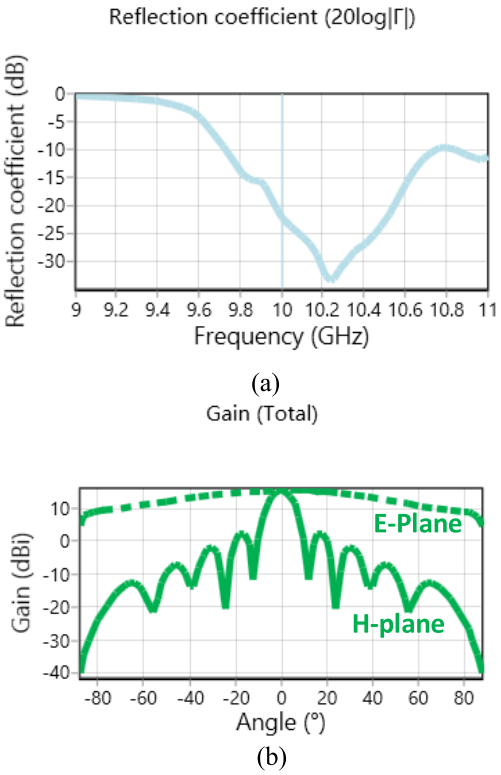

FIGURE 4. Characteristics of designed antenna. (a) S11 parameter. (b) Gain of antenna in E and H planes.

The reflection coefficient of designed resonant series-fed patch array is shown in Fig. 4(a), it is observed to reach less than −10dB over the band of 9.75-10.75 GHz. The gain of antenna is 18dBi in 10GHz as shown in Fig. 4(b). On the E-plane, the antenna gain should be as large as possible to maintain the desired retro-reflectivity. By adjusting the width of rectangular patchs, the side lobes reduced to 15dB smaller than the main lobe. On the H-plane, there is a relative consistent gain in a large range of incident angles and it is desirable in the design because oblique incident is the key of van-atta array as it allows for the RCS of the array to be distinguished from that of the flat metal ground plane, which is a unique feature to the overall design.

B. EQUAL ELECTRICAL LENGTH TRANSMISSION LINE

In the design of van-atta array, the symmetrical antennas are connected by equal electrical length transmission line. To reduce the radiation loss and cross talk effects between adjacent lines, the ground coplanar waveguide(GCPW) line are applied for the van-atta network. The GCPW line is composed of a ground-plane on the back of PCB board and a coplanar waveguide(CPW) line on the surface of PCB board as shown in Fig. 5. The CPW is composed of the middle signal line and the ground plane on both sides. And two semi-infinite ground plates of CPW is connected with back groundplane through via holes.

The lengths of the transmission lines connecting the antennas are equal or integer multiples of the wavelength difference. In order to reduce the transmission line loss, use

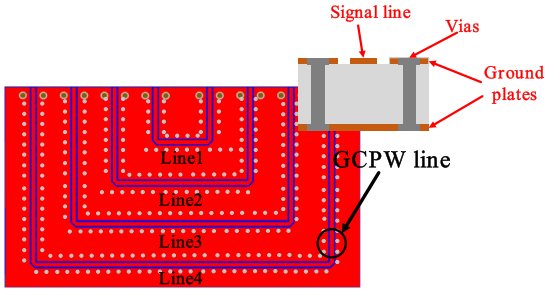

FIGURE 5. Schematic diagram of van-atta retro-reflective array.

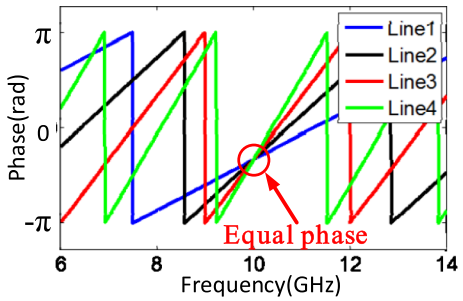

FIGURE 6. Schematic diagram of van-atta retro-reflective array.

a shorter transmission line, and the length of each transmission line differs by an integer number of wavelengths. The length of four GCPW lines $4\lambda_g$, $7\lambda_g$, $10\lambda_g$ and $13\lambda_g$. The phase delay of the 4 transmission lines in difference frequency is shown in Fig. 6. The four GCPW lines achieve same phase delay at frequency of $10GHz$.

C. VAN-ATTA ARRAY RCS

The 8 resonant series-fed rectangular microstrip patch arrays connected with 4 GCPW lines makes up the van-atta array. The overall of van-atta array and the RCS of it in different directional are shown in Fig. 7. In order to get the RCS of designed van-atta array in different direction, far-field plane wave in different incident angle is adopted as the source of energy excitation. The equivalent RCS can be calculated from the power of the echo signal in the direction of the incident wave. As shown in Fig. 7(a), the incident signal utilizes linear polarized wave and the polarization direction is identical to the array antennas.

Fig7(b) shows the RCS of designed van-atta array in different direction. To indicate the direction retro-reflection characteristics and its effect to the RCS of the van-atta array, RCS in different directions of the same size flat metallic plate is included for comparison. The van-atta array has the same RCS as the flat metal plate at vertical incidence of plane wave. However, as the oblique incidence angle of the plane wave increases, the RCS of the metal plate rapidly decays in the incident direction due to the specular reflection. The van-atta array can return the incident signal in the original direction due to its retro-reflection characteristics, thus can maintain a relatively large RCS in oblique incidence of plane wave.

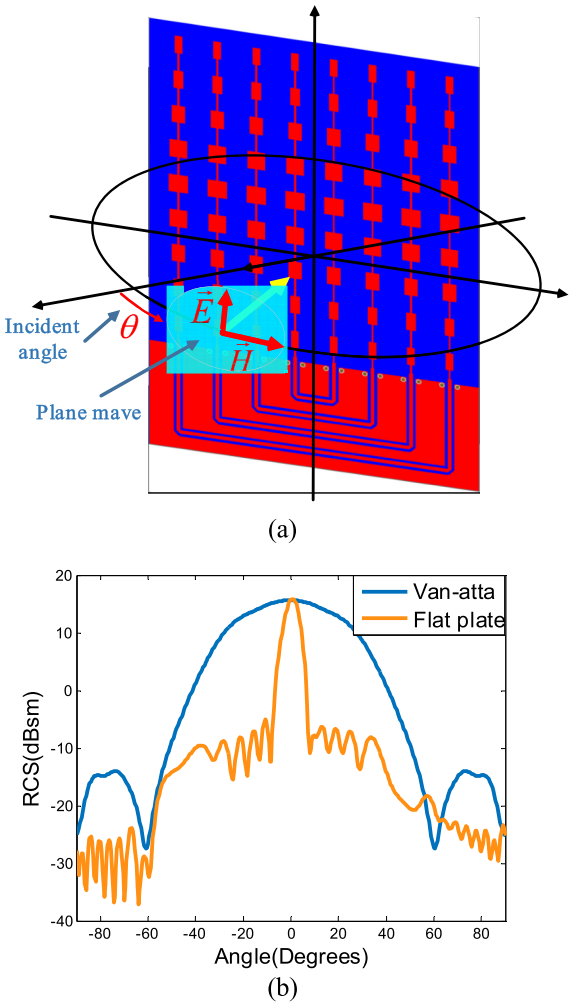

FIGURE 7. Schematic diagram of van-atta retro-reflective array.

As shown in Fig. 7(b), the RCS disparity between the van-atta array and the flat metallic plate under oblique incidence is mainly in the range of $-10°$ to $-40°$, where RCS of van-atta array is at least 10dB more than flat metallic plate.

IV. PHASE MODULATION OF RETRO-REFLECTED SIGNAL

In section III, the van-atta array is designed. The designed mocrostrip van-atta array has a relatively good retro-reflective performance in oblique signal incidence. To add phase modulation to the retro-reflected signal, in this section, a novel mocrostrip microwave single-pole double-throw (SPDT) switch is designed and incorporated in the interconnection line of van-atta array as mentioned in section II. The SPDT switch provide the retro-reflected signal ability of switching between two transmission lines separating half a wavelength. As a result, the phase of retro-reflected signal can be precisely switched from 0 to π by applying bias voltage to the SPDT switch.

The principle of microwave SPDT switch is shown in Fig. 8, the two PIN diodes are respectively connected $\lambda/4$ away from the branch in parallel. If the diode D1 is

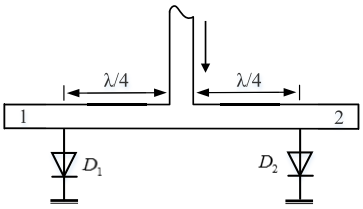

FIGURE 8. Principle of microwave single-pole double-throw (SPDT) switch.

conducted and the diode D2 is reversed, the channel 1 is short-circuited and no power is passed. Channel 2 does not affect power passing through because D2 is in an open-route state. Since D1 is λ/4 away from the branch, when D1 is short-circuited, the equivalent impedance of channel 1 to the branch is inf, so power transmission to channel 2 is not affected. Conversely, when diode D2 is conducted and diode D1 is reversed, power is transferred to channel 1, channel 2 is turned off, and channel 2 does not affect the power transmission to the channel 1.

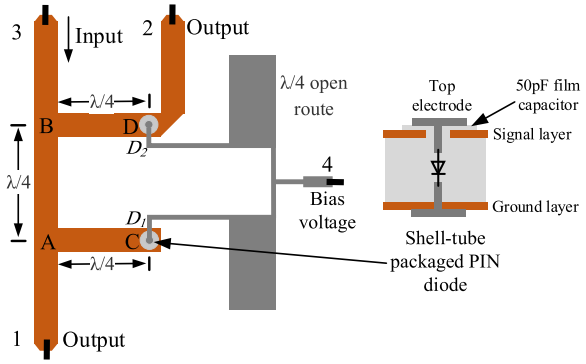

FIGURE 9. Design of mocrowave SPDT switch using microstrip line and PIN diode.

To turn one channel and another channel off, the two PIN diodes are always in opposite state, and two bias sources are required to control the two diodes. Actually, the SPDT switch always turns one channel on and another channel off, thus the two bias sources are always in the opposite state. To simplify the circuit and save the bias source, additional λ/4 branch is included to make the two diodes share one bias source. The mocrostrip SPDT switch circuit is shown in Fig. 9. Port 1, 2 are the two branch output channels, port 3 is the input channel, and port 4 is the input controlling bias source. In order to make D_1 and D_2 share one bias source, the diode D_1 originally connected to A point in parallel is replaced by a λ/4 length branch line from A point, and the diode is connected in parallel at terminal point C of the branch line, and diode D2 is still connected in parallel in point D of channel 2 which is λ/4 away from branch point B.

Shell-tube packaged PIN diode is suitable for parallel conjunction of microstrip line in parallel. As shown in Fig. 9, the PIN diode is embedded in the medium layer of the PCB, and the two electrodes are respectively connected to the top and bottom layers of the PCB. The anode electrode of the shell-tube PIN diode does not conduct to the microstrip line directly, and a 50pF capacitor series connection is formed by the top electrode, dielectric film and microstrip signal layer. Therefore, the top electrode of the PIN diode is separated from microstrip line in DC or low frequency and is conducted in high frequency, which is easy to apply a control bias voltage to the top electrode of the PIN diode.

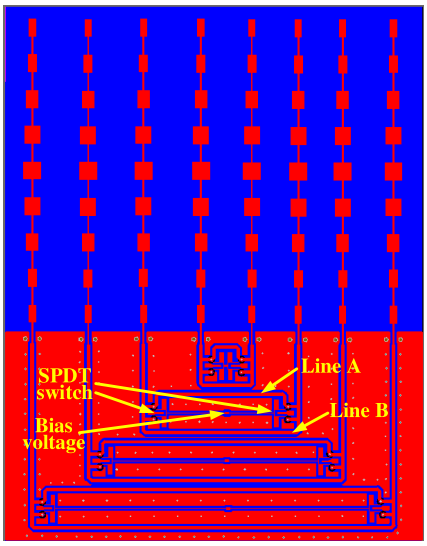

FIGURE 10. Overall design of van-atta array with SPDT switch to realize phase modulation.

The general design of the van-atta array with SPDT switch is shown in Fig. 10. Two SPDT switches are symmetrically connected to the transmission line, separating the 4 interconnected transmission lines of van-atta array to A and B branches respectively. The electrical length of the B branch is λ/2 longer than that of A branch. The two symmetrical switches of each transmission line share a bias source. When the bias voltage is off, the line A is connected, and when the bias voltage is on, the line B is connected. By controlling the on and off of the bias source, the backtracking signal can be transmitted from two different transmission lines.

The 4 bias voltages control the 4 circuits respectively. To maintain the same electrical length of 4 circuits, the 4 bias voltages share the same state. The phase delay of 4 circuits in bias voltage on and off is shown in Fig. 11. While bias voltage is off, the 4 circuits attain same phase delay of 0.67π at 10GHz. And while bias voltage is on, the phase delay attains to -0.33π, which is delayed π rad more than that of bias voltage off. As analyzed in section II, by controlling the phase delay from 0 to π, the signal phase is reversed and reflection coefficient of the retro-reflected signal is altered from 1 to -1. Using a periodical rectangular waveform as the bias voltage can realize periodic phase modulation of the retro-reflected signal. That means, the retro-reflected signal is modelated by square signal $p(t)$, the $p(t)$ can be

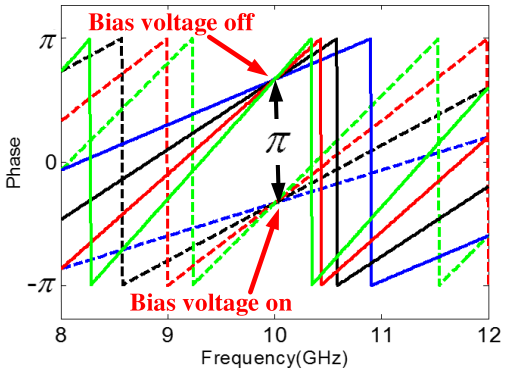

FIGURE 11. Phase delay of 4 circuits in bias voltage on and off state.

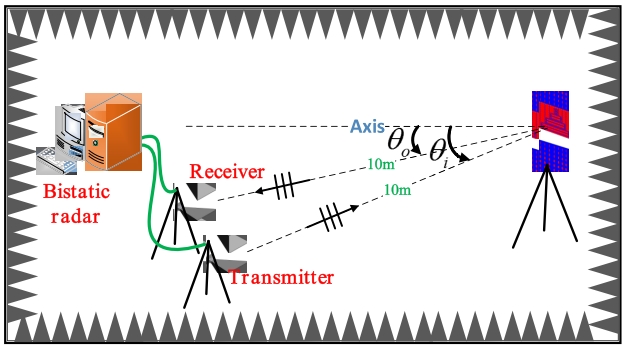

FIGURE 12. Scenes Using square waveform to realize the ±1 of van-atta array retro-reflection coefficient.

expressed as:

$$p(t) = rect_{\pm 1}\left(\frac{t}{\tau T_s}\right) \otimes \delta_n(t - nT_s) \tag{3}$$

where τ is the duty cycle of modelating signal, T_s is the period of modelating signal, the $\otimes$ represents the convolution operation, $\delta_n(\cdot)$ represents the discrete impulse function.

The $p(t)$ can also be expressed using Fourier series as:

$$p(t) = A_0 + \sum_{n=1}^{\infty} 2A_n \cos(2\pi n f_s t) \tag{4}$$

where $A_0 = 2\tau$-1, A_n =(1-cos($2n\pi\tau$))/$n\pi$. When $\tau = 0.5$, $p(t)$ is square waveform. Then $A_0 = 0$, the $A_n = 1$ when n = odd and $A_n = 0$ when n = even. The $p(t)$ can also be expressed as:

$$p(t) = \sum_{n=odd} \frac{2}{n\pi} \cos(2\pi n f_s t) \tag{5}$$

where f_s is the frequency of modulation signal and $f_s = 1/T_s$. Frequency spectrum $P(f)$ of $p(t)$ is:

$$P(f) = \sum_{\substack{n=-\infty \\ n\neq 0}}^{+\infty} \mathrm{sinc}(n\pi/2) \cdot \delta(f - nf_s) \tag{6}$$

where sinc(·)= sin(·)/(·). While the incident signal $s(t)$ is modulated by $p(t)$, the retro-reflected signal $s_r(t)$ can be seen as multiplying the incident signal with the modulated signal, it can be expressed as:

$$s_r(t) = s(t) \cdot p(t) \tag{7}$$

According to the Fourier transform, multiplication of signals in the time domain is equivalent to convolution in the frequency domain. Therefore, the frequency spectrum of $s_r(t)$ is:

$$\begin{aligned} S_R(f) &= S(f) \otimes P(f) \\ &= \sum_{\substack{n=-\infty \\ n\neq 0}}^{+\infty} \mathrm{sinc}(n\pi/2) \cdot S(f - nf_s) \end{aligned} \tag{8}$$

where $S(f)$ is the frequency spectrum of incident signal $s(t)$. According to formula (8), the modulated retro-reflected signal can be easily distinguished from incident signal. Whose frequency spectrum is the frequency spectrum $S(f)$ extended in the frequency domain with f_s, the amplitude envelope of spectrum is sinc(·), and the frequency interval of adjacent two sidebands in the frequency domain is $2f_s$.

V. RETRO-REFLECTIVE CHARACTERISTIC MEASUREMENT OF VAN-ATTA ARRAY

In this section, the van-atta array is tested in microwave anechoic chamber, the bistatic radar is applied to measure the high-resolution range profile of van-atta array in different angle.

The bistatic radar system using LFM signal as its transmitting signal, and the parameters of radar system are: carrier frequency $f_c = 10.24GHz$ ($\lambda_c \approx 2.9cm$), signal bandwidth $B_w = 500MHz$, pulse duration $T_p = 12.8\mu s$, and chirp rate $K_r = 39.1GHz/ms$. Matched filter is adopted to fulfill pulse compression and get the high-resolution range profile of designed van-atta array. As shown in Fig. 12, the angle of transmitter and receiver to axis of van-atta array are θ_i and θ_o and counterclockwise direction is taken as the positive direction. The transmitter and receiver are both 10 meters away from the van-atta array.

In order to distinguish the high-resolution range profile between retro-reflected signal and the specular reflection signal of designed van-atta array, the square waveform with frequency $f_s = 0.75MHz$ is adopted as the van-atta array bias voltage. Thus the phase of retro-reflected signal is delayed between 0 and π periodically, which is equal to reflection coefficient of retro-reflected signal switching between 1 and -1 periodically. According to the analysis in section IV, the frequency spectrum of modulated retro-reflected signal is a series sidebands spectrum of incident signal and interval of adjacent two sidebands in the frequency domain is $2f_s$. After compression by matched filter, the compressed echo of phase modulated signal in high-resolution range profile is a series of false targets with the interval $\Delta r = 2cf_s/K_r$. The false targets deviate the position of real target, symmetrically distributed the two sides of real target, and the false targets decrease

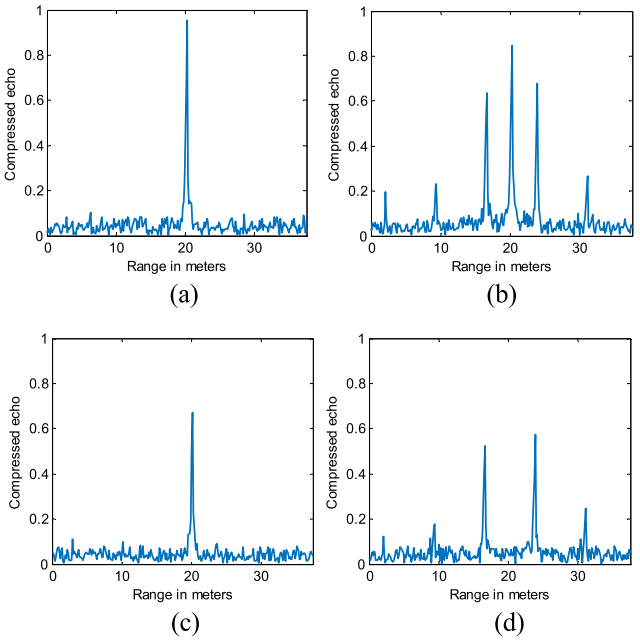

FIGURE 13. The compressed echo of van-atta array in different angle and modulation. (a) $\theta_i = \theta_o = 0°$, bias voltage off. (b) $\theta_i = \theta_o = 0°$, bias voltage square wave modulated. (c) $\theta_i = 15°$, $\theta_o = 15°$, bias voltage off. (d) $\theta_i = 15°$, $\theta_o = 15°$, bias voltage square wave modulated.

with the distance away from the real target increases. The high-resolution range profile of designed van-atta on different angle is shown in Fig. 13.

While angle of transmitter and receiver is 0° ($\theta_i = \theta_o = 0°$), the radar signal incidents vertically to the van-atta array. The received signal contains two parts, specular reflected signal and retro-reflected signal. As shown in Fig. 13(a), while the bias voltage is off, the retro-reflected signal is similar as specular reflected signal with only a tiny delay. Since the radar has not enough resolution power to distinguish them, there is only one target in high-resolution range profile. While the square wave is adopted as the bias source, the retro-reflected signal is attached with intermittent periodic phase modulation. As a result, the high resolution range profile of retro-reflected signal is a series of false targets symmetrically distributed on both sides of the real position of van-atta array. Since the specular reflected signal maintains unchanged, the range profile of it is still in the original position, so it can be easily separated from range profile of the retro-reflected signal as shown in Fig. 13(b).

When the transmitter and receiver are on the same position and they are both 30° oblique to the axis of van-atta array ($\theta_i = \theta_o = 15°$), the angle of specular reflected signal is $-15°$ and it can not be received. Only retro-reflected signal can return in the direction of the incident signal and be detected by the receiver. Fig. 13(c) shows the high resolution range profile of retro-reflected signal. While the square wave is adopted as the bias source, the range profile of retro-reflected signal is separated to several symmetrical false targets. The interval of false targets is $\Delta r = 11.5m$, which is in accordance with the theoretical analysis presented before.

VI. CONCLUSION

In this paper, a phase adjustable microstrip van-atta array with SPDT switch is designed. The designed van-atta array can maintain a relatively large RCS in the wide angle range and phase modulation is realized with incorporation of the microwave SPDT switches into the transmission line. Through controlling the on and off state of the bias voltage, the phase delay of retro-reflected signal can be precisely switch from 0 to π. The phase modulation characteristic of designed van-atta array is tested in microwave anechoic chamber, and the result implies that modulated van-atta array has a great potential for radar jamming system and it can be used to generate multiple false targets in high-resolution range profile of radar.

REFERENCES

[1] D. Feng, L. Xu, X. Pan, and X. Wang, "Jamming wideband radar using interrupted-sampling repeater," *IEEE Trans. Aerosp. Electron. Syst.*, vol. 53, no. 3, pp. 1341–1354, Jun. 2017.

[2] S. B. S. Hanbali and R. Kastantin, "Technique to counter active echo cancellation of self-protection ISRJ," *Electron. Lett.*, vol. 53, no. 10, pp. 680–681, May 2017.

[3] Q. Wu, F. Zhao, X. Ai, X. Liu, and S. Xiao, "Two-dimensional blanket jamming against ISAR using nonperiodic ISRJ," *IEEE Sensors J.*, vol. 19, no. 11, pp. 4031–4038, Jun. 2019.

[4] C.-Z. Li, W.-M. Su, H. Gu, C. Ma, and J.-L. Chen, "Improved interrupted sampling repeater jamming based on DRFM," in *Proc. IEEE Int. Conf. Signal Process., Commun. Comput. (ICSPCC)*, Guilin, China, Aug. 2014, pp. 254–257.

[5] H.-X. Huang, Z.-T. Huang, and Y.-Y. Zhou, "Jamming research to SAR based on frequency characteristic," in *Proc. 2nd Int. Conf. Signal Process. Syst.*, Dalian, China, Jul. 2010, pp. V2-144–V2-147.

[6] L. Xu, D. Feng, and X. Wang, "Improved synthetic aperture radar micro-Doppler jamming method based on phase-switched screen," *IET Radar, Sonar Navigat.*, vol. 10, no. 3, pp. 525–534, Mar. 2016.

[7] J. Wang, D. Feng, L. Xu, and W. Hu, "Synthetic aperture radar image modulation using phase-switched screen," *IEEE Antennas Wireless Propag. Lett.*, vol. 17, no. 5, pp. 911–915, May 2018.

[8] J. Wang, D. Feng, Q. Wu, L. Xu, and W. Hu, "Synthetic aperture radar target feature transformation method based on random code phase-switched screen," *IEEE Access*, vol. 6, pp. 41173–41178, 2018.

[9] K. S. B. Yau, "Planar multi-layer passive retrodirective Van Atta array reflectors at X-band," in *Proc. Int. Symp. Antennas Propag. (ISAP)*, Hobart, TAS, Australia, Nov. 2015, pp. 1–4.

[10] F. Farzami, S. Khaledian, B. Smida, and D. Erricolo, "Reconfigurable dual-band bidirectional reflection amplifier with applications in Van Atta array," *IEEE Trans. Microw. Theory Techn.*, vol. 65, no. 11, pp. 4198–4207, Nov. 2017.

[11] H. I. El-Sawaf, A. M. El-Tager, and A. M. Ghuneim, "A proposed 2-D active Van Atta retrodirective array using dual-polarized microstrip antenna," in *Proc. Asia–Pacific Microw. Conf.*, Dec. 2012, pp. 1103–1105.

[12] M. Ettorre, W. A. Alomar, and A. Grbic, "2-D Van Atta array of wideband, wideangle slots for radiative wireless power transfer systems," *IEEE Trans. Antennas Propag.*, vol. 66, no. 9, pp. 4577–4585, Sep. 2018.

[13] J. Vitaz, A. Buerkle, and K. Sarabandi, "Tracking of metallic targets using a retro-reflective array at 26 GHz," in *Proc. IEEE Antennas Propag. Soc. Int. Symp.*, Charleston, SC, USA, Jun. 2009, pp. 1–4.

[14] K. W. Kobayashi, L. Tran, A. K. Oki, and D. C. Streit, "A 50 MHz-30 GHz broadband co-planar waveguide SPDT PIN diode switch with 45-dB isolation," *IEEE Microw. Guided Wave Lett.*, vol. 5, no. 2, pp. 56–58, Feb. 1995.

[15] S.-H. Park and Y.-W. Choi, "Significantly enhanced isolation of SPDT switch using punched hole structure," *IEEE Microw. Wireless Compon. Lett.*, vol. 13, no. 2, pp. 75–77, Feb. 2003.

[16] Y. Ushijima, E. Nishiyama, and M. Aikawa, "Single layer extensible microstrip array antenna integrating SPDT switch circuit for linear polarization switching," *IEEE Trans. Antennas Propag.*, vol. 60, no. 11, pp. 5447–5450, Nov. 2012.

[17] K. Ichihashi, K. Sakakibara, and N. Kikuma, "Bandwidth comparison of traveling-wave and standing-wave array designs of series-fed microstrip patch array antennas," in *Proc. IEEE Int. Workshop Electromagn., Appl. Student Innov. Competition*, Nagoya, Japan, Aug. 2018, p. 1.
[18] Z. Chen and S. Otto, "A taper optimization for pattern synthesis of microstrip series-fed patch array antennas," in *Proc. Eur. Wireless Technol. Conf.*, Rome, Italy, Sep. 2009, pp. 160–163.
[19] J.-P. Raskin, G. Gauthier, L. P. Katehi, and G. M. Rebeiz, "Mode conversion at GCPW-to-microstrip-line transitions," *IEEE Trans. Microw. Theory Techn.*, vol. 48, no. 1, pp. 158–161, Jan. 2000.
[20] M. El-Gibari, D. Averty, C. Lupi, M. Brunet, H. Li, and S. Toutain, "Ultra-broad bandwidth and low-loss GCPW-MS transitions on low-k substrates," *Electron. Lett.*, vol. 46, no. 13, pp. 931–933, Jun. 2010.

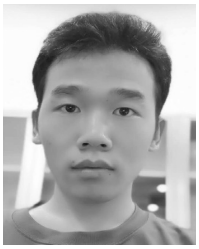

KUNPENG SONG was born in Xiangyang, Hubei, China, in 1994. He received the B.S. degree in electronic engineering from the National University of Defense Technology, Changsha, China, in 2017, where he is currently pursuing the M.S. degree with the State Key Laboratory of Complex Electromagnetic Environmental Effects on Electronics and Information System. His research interests include radar signal processing and radar jamming.

DEJUN FENG was born in Hunan, China, in 1972. He received the M.S. degree from the Naval University of Engineering, Nanjing, China, in 2002, and the Ph.D. degree from the National University of Defense Technology, Changsha, China, in 2006, respectively, where he is currently an Associate Professor. His research interests include radar signal processing, radar system simulation, and inverse synthetic aperture radar.

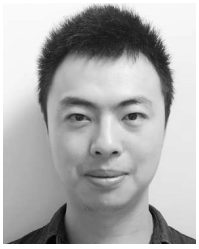

JUNJIE WANG was born in Hunan, China, in 1991. He received the B.S. degree in communication engineering from Hunan University, Changsha, China, in 2014, and the M.S. degree in information and communication engineering from the National University of Defense Technology, Changsha, China, in 2016, where he is currently pursuing the Ph.D. degree with the State Key Laboratory of Complex Electromagnetic Environmental Effects on Electronics and Information System. His research interests include radar imaging and radar signal processing.

QIANPENG XIE was born in Henan, China, in 1991. He received the B.S. and M.S. degrees from the Electronic Engineering Institute, Hefei, China, in 2014 and 2016, respectively. He is currently pursuing the Ph.D. degree with the National University of Defense Technology. His research interests include array signal processing, radar signal processing, and electromagnetic environment effects.

LEI LIU was born in Guangdong, China, in 1994. She received the B.S. degree in communication engineering from Hunan University, Changsha, China, in 2017. She is currently pursuing the M.S. degree with the State Key Laboratory of Complex Electromagnetic Environmental Effects on Electronics and Information System, National University of Defense Technology. Her research interests include passive radar jamming and radar signal processing.